Biophysical Drivers of Coastal Treeline Elevation

G. D. Molino[1], J. A. Carr[2], N. K. Ganju[3], and M. L. Kirwan[1]

[1]Virginia Institute of Marine Science, William & Mary, Gloucester Point, VA, United States.

[2]U.S. Geological Survey, Eastern Ecological Science Center, Beltsville, MD, United States.

[3]U.S. Geological Survey, Woods Hole Coastal and Marine Science Center, Woods Hole, MA, United States.

Corresponding author: Grace D. Molino (gdmolino@vims.edu)

Key Points:

- Treeline elevations increase with tidal range, salinity and slope, but are not correlated with climate or marsh characteristics
- Macro-scale drivers account for <50% treeline elevation variability indicating that local factors mediate estuary-scale sea level responses
- Offset between treeline elevation and tidal datums suggest that standard sea level rise projection methods may misrepresent land conversion

Abstract

Sea level rise is leading to the rapid migration of marshes into coastal forests and other terrestrial ecosystems. Although complex biophysical interactions likely govern these ecosystem transitions, projections of sea level driven land conversion commonly rely on a simplified 'threshold elevation' that represents the elevation of the marsh-upland boundary based on tidal datums alone. To determine the influence of biophysical drivers on threshold elevations, and their implication for land conversion, we examined almost 100,000 high-resolution marsh-forest boundary elevation points, determined independently from tidal datums, alongside hydrologic, ecologic, and geomorphic data in the Chesapeake Bay, the largest estuary in the U.S. located along the mid-Atlantic coast. We find five-fold variations in threshold elevation across the entire estuary, driven not only by tidal range, but also salinity and slope. However, more than half of the variability is unexplained by these variables, which we attribute largely to uncaptured local factors including groundwater discharge, microtopography, and anthropogenic impacts. In the Chesapeake Bay, observed threshold elevations deviate from predicted elevations used to determine sea level driven land conversion by as much as the amount of projected regional sea level rise by 2050. These results suggest that local drivers strongly mediate coastal ecosystem transitions, and that predictions based on elevation and tidal datums alone may misrepresent future land conversion.

Plain Language Summary

As sea level rise (SLR) drives saltwater further inland, terrestrial ecosystems change to tidally-controlled ecosystems. A common ecosystem transition is coastal forest conversion to marsh, which forms ghost forests, characterized as dead trees surrounded by marsh. Most projections of (SLR) assume that the boundary between forest and marsh can be defined simply by the furthest

landward extent of the tide. However, forest to marsh conversion can be influenced by other physical processes and vegetation interactions. Here we analyze the location of the marsh-forest boundary across the entire Chesapeake Bay, defined using 100,000 elevation points, alongside environmental variable datasets to determine drivers of coastal forest retreat. As the largest estuary in the U.S., the Chesapeake Bay provides a study area where the elevation of transition from forest to marsh varies substantially. We find this variation in elevation to be driven by not only tidal range, but also soil salinity and slope of the land, yet these variables explain <50% of the variability in elevation. This suggests that local factors unaccounted for in this study also strongly influence the retreat of coastal forests, even at regional scales. Therefore, projections of SLR that rely solely on tidal extents may misrepresent future land conversion.

1 Introduction

Sea level rise is leading to rapid transformation of coastal ecosystems, where barrier islands, marshes, and coastal forests are all migrating inland to higher elevations (E. E. White et al., 2021; Zinnert et al., 2019). These ecosystems are arranged in patterns largely set by elevation relative to position within the tidal frame (Brinson et al., 1995; Oertel, 1985). However, the elevation of transition from marsh to coastal forest, or threshold elevation, deviates from what is expected based on tidal datums due to complex interactions between other physical and biotic variables (Boon et al., 1977). Climate change adds a global-scale driver of threshold elevation as accelerating rates of global sea level rise (SLR) shift the marsh-forest boundary landward, but it remains unclear how local variables will interact to mediate the degree of change (Poulter et al., 2009; Robichaud & Begin, 1997).

Untangling the interactions between global drivers and local factors is central to understanding the process of upland conversion to marsh. Increased tidal flooding from SLR is

well established as a dominant global-change mechanism controlling marsh migration into retreating coastal forests (Wasson et al., 2013; Williams et al., 1999). Saturated soils create hypoxic conditions which can result in reduced root conductance and eventually mortality of the roots (McDowell et al., 2022). Root mortality reduces water uptake by the tree, leading to loss of the tree crown and carbon starvation (McDowell et al., 2022). Saltwater intrusion, which can accompany SLR, has similar effects on tree mortality (McDowell et al., 2022). The osmotic potential of saline pore water is higher than the root water potential of most woody coastal taxa, which can reduce or eliminate the flow of water into roots (McDowell et al., 2022). Most seedlings and saplings are unable to tolerate even brief inundation by saline water, preventing forest regeneration years before mature trees die (Brinson et al., 1995; Williams et al., 1999). Salt spray during storms can further limit trees to elevations higher than those regularly inundated from tides (Boon et al., 1977; Robichaud & Begin, 1997). Saturated soils and salt-stress increase forest vulnerability to disturbance events, such as storms, which are responsible for large-scale forest dieback events (Ury et al., 2021).

Global-change drivers of tree mortality are mediated by local conditions at the marsh-forest boundary, and its position within the larger coastal landscape. On a landscape-scale, the marsh-forest ecotone is assumed to migrate inland faster in gently sloping areas (Brinson et al., 1995; Fagherazzi et al., 2019; Kirwan et al., 2016). Marsh-forest ecotones within low slope environments are more regularly inundated and generally have smaller watershed drainage areas, limiting freshwater inputs that would otherwise reduce salt accumulation (Hussein, 2009; Hussein & Rabenhorst, 2001). High slope environments facilitate better drainage of the marsh-forest ecotone (Brinson et al., 1995). The distance from the treeline to water could also potentially influence retreat of the coastal forest. Both flood extent inland and subsurface

salinization decrease with increasing distance from open water to uplands (Guimond & Michael, 2021), as wider marshes reduce exposure of the marsh-forest ecotone to storm surge and mitigate saltwater intrusion. Less permeable systems, such as those with clay-rich soils, reduce drainage after inundation events, and thus increase root exposure to saline and/or hypoxic conditions (Nordio et al., 2023). Shallow groundwater tables support saturated soil conditions and reduced seaward groundwater flow with SLR (Guimond et al., 2020), which can extend the time it takes saltwater pulses from storms to dissipate, increasing the likelihood of tree mortality. Terrestrial vegetation is primarily limited by abiotic factors (Veldkornet et al., 2015), but species-specific interactions mediate the responses to macro-scale drivers. Biotic factors such as shading, recovery from disturbance, and tree-specific adaptations such as symmetric root distribution all likely influence the conversion of uplands to marsh (Field et al., 2016; Messerschmidt et al., 2021; Poulter et al., 2009; Veldkornet et al., 2015). Therefore, the response of the forest-marsh ecotone is controlled by the interplay between global change and local variables.

Maintenance of tidal marsh ecosystems, and the habitat provision, carbon sequestration, and water quality services they provide (Brittain & Craft, 2012; Craft et al., 2009; A. J. Smith & Kirwan, 2021), will rely upon upland conversion to marsh at a global scale (Schuerch et al., 2018). However, most marsh migration projections assume that the marsh-forest boundary occurs at an elevation that can be approximated by a tidal datum (e.g. mean higher high water) (Buchanan et al., 2022; Doyle et al., 2010; Holmquist et al., 2021; Mitchell et al., 2020; Osland et al., 2022; Warnell et al., 2022), despite the understanding that the lower limit of coastal forests is driven by a range of biophysical factors beyond tides. Here, we examine the elevation of independently delineated, high-resolution marsh-forest boundary points in the Chesapeake Bay, located along the U.S. mid-Atlantic coast, alongside biological and physical datasets to assess

key drivers of coastal treeline elevation at the watershed scale. We interpret these 'threshold elevations' as reflecting the cumulative influence of drivers that affect the survival of coastal forests, allowing us to demonstrate that local factors strongly mediate global change driven patterns of ecosystem migration.

2 Materials and Methods

2.1 Study area

We investigated the biophysical controls of marsh-forest boundary by examining threshold elevations in the Chesapeake Bay region, a hotspot for sea level driven forest retreat (Schieder & Kirwan, 2019). Approximately 400 km^2 of uplands have converted to marsh since the late 19^{th} century (Schieder et al., 2018), with rates of retreat that are accelerating in parallel with rates of sea level rise (Schieder & Kirwan, 2019). The average rate of relative sea level rise has increased from 2.45 mm yr^{-1} (1953 to 1983) to 4.7-6.2 mm yr^{-1} (1975 to 2021) (Ezer, 2023; Ezer & Atkinson, 2015). Concurrent with accelerating sea level rise rates, coastal forests migrated upslope and horizontal forest retreat rates accelerated from 3.1 m yr^{-1} (1985–2000) to 4.7 m yr^{-1} (2001–2020) in a portion of the Chesapeake Bay (Chen & Kirwan, 2022a). By 2100, 1050-3748 km^2 of uplands are projected to convert to marsh, largely at the expense of terrestrial forests and freshwater forested wetlands (Molino et al., 2022).

Low elevation terrestrial forests adjacent to marshes in this region typically include loblolly pine (*Pinus taeda*) and Eastern red cedar (*Juniperus virginiana*) (Perry et al., 2001), with forested wetlands commonly comprised of swamp tupelo (*Nyssa biflora*) and red maple (*Acer rubrum*) (Noe et al., 2021). High marsh is usually composed of saltmeadow cordgrass (*Spartina patens*), saltgrass (*Distichlis spicata*), and black needlerush (*Juncus romerianus*) (Perry et al.,

2001; U.S. Fish and Wildlife Service, 2018). The invasive common reed, *Phragmites australis,* is commonly found at the marsh-forest boundary as a sign of disturbance and ecosystem conversion (Jobe IV & Gedan, 2021; Langston et al., 2021; Shaw et al., 2022; J. A. M. Smith, 2013).

Marshes in this region are highly vulnerable to sea level rise as a result of reduced sediment supply and limited tidal influence (Noe et al., 2020; Xiong & Berger, 2010). Almost 200 km^2 of marsh has been lost across the Chesapeake and Delaware Bays over the past 40 years (Chen & Kirwan, 2022b). Marsh fragmentation and drowning continues to be a concern for Chesapeake Bay marshes given their limited vertical accretion potential (Duran Vinent et al., 2021; M. S. Kearney et al., 2002). Marsh migration into upland forests has historically compensated for erosion of marshes in the region (Chen & Kirwan, 2022b; Schieder et al., 2018). Therefore, understanding drivers of coastal forest retreat is critical to improving projections of future marsh area.

2.2 Input variables

The high-resolution (30 m) threshold elevation dataset was comprised of >95,000 points aggregated into median threshold elevations for 81 watersheds within Chesapeake Bay and adjacent coastal lagoons (Figure 1, Supporting Information Figure S1) (Molino et al., 2022), which allows for comparison with watershed-scale environmental variables. Marsh-forest boundary location was determined using a spatially explicit approach, independent of tidal datums (Molino, Defne, et al., 2021), in contrast to other approaches (ex. Holmquist et al., 2021; Warnell et al., 2022). Threshold elevation values were extracted at each elevation point from U.S. Geological Survey (USGS) Coastal National Elevation Database (CoNED) Topobathymetric Digital Elevation Model (Danielson & Tyler, 2016), a high-resolution (1 m)

aggregate of elevation datasets published between 2004 and 2016. Preparation of additional spatially-explicit environmental datasets for this study was completed in geographic information software (ArcGIS Desktop 10.7) (Table 1).

We analyzed 14 environmental factors that were predicted to control rates of coastal forest dieback alongside previously determined marsh-forest boundary elevations (Table 1) (Molino et al., 2023). Hydrologic, topographic, climactic, and disturbance input variables were identified based on previously documented relationships with threshold elevation, marsh migration likelihood, or coastal forest retreat (Table 1). Values for predictor environmental variables were extracted at the original threshold elevation points and then aggregated into median values by watershed (Figure 2; Supporting Information Figures S2-13). The spatial extent of some datasets did not cover all threshold elevation points so in those cases a subset of points was used to calculate the median value for the watershed. Median values for datasets with low resolution (temperature, precipitation, growing degree days) or for datasets which did not extend to the marsh-forest boundary (salinity, tidal range) were determined from the environmental variable data points which fell within each watershed.

We incorporated tidal range, salinity, surface water occurrence, change in surface water occurrence, and normalized difference water index (NDWI) data to analyze the influence of hydrology on forest retreat. Tidal range was calculated as the difference between Mean High Water and Mean Low Water, provided for the entire U.S. coastline at 400 m resolution by the National Oceanic and Atmospheric Administration's (NOAA) vertical datum transformation tool (VDatum). Surface salinity data were modeled by St-Laurent et al., (2020) for the Chesapeake Bay and Atlantic coastal lagoons. Surface water occurrence is the percentage of water detections from March 1984 to December 2020 and change in surface water occurrence is the percent

difference in water occurrence between 1984-1999 and 2000-2020 (Pekel et al., 2016). Mean NDWI was computed from near infrared (NIR) and shortwave-infrared (SWIR1) bands available from Landsat-8 imagery acquired from USGS Earth Explorer from June through August 2016-2020 using the formula NDWI = (NIR – SWIR1)/(NIR + SWIR1) (Chen & Kirwan, 2022b). Unique NDWI values were extracted at each marsh-forest boundary point.

To determine the influence of topography on tree mortality, we quantified slope, topographic position index (TPI), watershed area, and distance to open water (Table 1) for each marsh-forest boundary point. Slope and TPI were derived from the USGS CoNED Topobathy (Danielson & Tyler, 2016). Slope was calculated as the average slope within 10 m on either of the marsh-forest boundary (Molino et al., 2020). TPI, which examines if a single cell is higher or lower than its surroundings (i.e. a hill vs gulley), was calculated using $TPI_i = y_m - y_i$ where y_m is the mean elevation of a 3x3 cell grid and y_i is the elevation of the central raster cell in the grid. Watershed area was determined by the area of the Hydrologic Unit (HUC) 10 watershed delineated by the USGS (USGS, 2020) and distance to open water was calculated as the Euclidean distance from the marsh-forest boundary point to water as delineated by the Chesapeake Conservancy Land Use (using the Near tool in ArcMap) (Chesapeake Conservancy, 2018).

Climate variables, including annual temperature, precipitation, and growing degree days were obtained from the PRISM Climate Group 4-km resolution datasets (Table 1) (PRISM Climate Group, Oregon State University, 2019). Annual growing degree days were derived from the temperature dataset as the number of days when the average temperature is greater than or equal to 10°C (Chen & Kirwan, 2022b). Each of these variables is calculated as the long-term mean from 1984 to 2020 and is incorporated in the model to examine how regional variation in

climate mediates forest response to sea level rise. To assess the influence of a hurricane on forest retreat, we extracted maximum inundation height (m) and inundation duration (hours) during Hurricane Isabel at each marsh-forest boundary point from the Advanced Circulation (ADCIRC) Prediction System (Molino, Defne, et al., 2021). Hurricane Isabel, which made landfall in September 2003, was selected as the most significant storm to affect the Chesapeake Bay since at least 1954 (Beven & Cobb, 2004). We therefore would expect this disturbance event to have the highest likelihood of promoting coastal forest retreat inland, such as resulted from a comparable storm in North Carolina (Ury et al., 2021).

2.3 Analytical approach

We used a linear model to assess the importance of biological and physical variables in controlling coastal treeline elevations (run in Python 3 using the statsmodels package). Due to data resolution limits, the linear model was run on the aggregated values of threshold elevation and predictor variables for each watershed. The areal overlap of all the datasets formed the extent of the analyses as all variables needed to be present in a watershed for it to be included in the model. We fit a linear regression model to explain the median threshold elevation for 68 watersheds within the Chesapeake Bay (Figure 2). The model started with 14 variables which we assessed for multicollinearity using a pairwise correlation matrix and variance inflation factors (VIF) (calculated in Python) (Zuur et al., 2009). Highly correlated variables (Pearson's r greater > 0.5) and those with a VIF above 5 were removed. The remaining variables were run in the model, followed with a backward stepwise selection whereby we eliminated insignificant variables until only significant variables remained. We calculated percent error for each watershed to validate the results of the model.

225 ### 2.4 Comparison to tidally determined threshold elevations

226 We quantified how three different methods of determining the marsh-forest boundary
227 alter threshold elevations as well as predictions of future marsh migration area: a single value for
228 the region (Mitchell et al., 2020), a tidal datum (NOAA Office for Coastal Management, 2019),
229 and our spatially explicit marsh-forest boundary delineations (Molino et al., 2022). To calculate
230 the difference in threshold elevation between a single, tidally-derived value and the spatially
231 explicit methods, we compared a single value for threshold elevation for Virginia approximated
232 from highest astronomical tide (HAT) (Mitchell et al., 2020), to unique threshold elevations for
233 each watershed determined by our marsh-forest boundary delineations (Molino et al., 2022).
234 Similarly, we extracted the value of mean higher high water spring (MHHWS) (Holmquist et al.,
235 2019) at each marsh-forest boundary point and compared the value to threshold elevations
236 created independently from current marsh and forest extents (Molino et al., 2022). To quantify
237 the predicted marsh migration area determined by the tidal datum method, we summed the total
238 upland area between the current marsh-upland boundary and the predicted Mean Higher High
239 Water (MHHW) level for the entire study area under two SLR scenarios (0.45 and 1.22 m by
240 2100). This tidal datum corresponds to the predicted landward extent of brackish/transition
241 marsh in NOAA's Office of Coastal Management Sea Level Rise Viewer (NOAA Office for
242 Coastal Management, 2019). We then compared the upland area predicted to convert based on
243 MHHW with the area predicted to convert to salt marsh under comparable SLR scenarios but
244 using both the single threshold value method (Mitchell et al., 2020) as well as independently
245 determined threshold elevations (Molino et al. 2022).

3 Results

The median of the 95,286 threshold elevation points in Chesapeake Bay is 0.54 m. Median threshold elevation for each watershed varies from 0.2 m North American Vertical Datum of 1988 (NAVD88) in the southernmost watersheds to 1.05 m NAVD88 in the Virginia Atlantic coastal lagoons (Figure 1). Simple linear regression revealed that tidal range and salinity had the best simple linear model fits with threshold elevation at the point and watershed scales (Figure 3). Threshold elevation increased significantly with tidal range, on the scale of individual points ($p<0.00001$) and watersheds ($p<0.0001$) (Figure 3). Threshold elevation similarly increased with salinity at point ($p<0.00001$) and watershed ($p<0.01$) scales (Figure 3). These relationships are consistent with probability distribution functions in paired representative watersheds, where two of the three variables (tidal range, salinity, slope) were held constant (Figure 4). For example, probability distribution functions of threshold elevations within watersheds with high tidal range (Metompkin) and low tidal range (Upper Chincoteague) display a positive skew of threshold elevation in the watershed with the higher tidal range (Figure 4b). These watersheds are located in a similar geographic area (Supporting Information Figure S1) and have similar median salinities (32.1 vs 32.2 ppt) and slopes (2.51 vs 2.62 %), suggesting that tidal range alone is responsible for the variation in threshold elevation.

The multiple linear regression explained 44% of the variability in threshold elevations at the watershed scale. The significant variables determined by the regression confirmed the relationship between threshold elevation and tidal range and salinity, with tidal range as the most important variable in determining threshold elevation at the watershed scale. However, the linear model also found that slope across the marsh-forest boundary is a significant variable (Table 1). Despite only having a significant relationship at the point ($p<0.00001$), not watershed ($p=0.14$)

scale, slope has a higher coefficient than salinity (Table 1). No other input variables had a significant relationship with threshold elevation.

Marsh-forest boundary threshold elevations obtained using a single value from a tidal datum (e.g. highest astronomical tide), under- or over-estimated spatially explicit threshold elevations by 0.29-0.44 m (Table 2). The most pronounced difference between the two methods is in the high tidal range Atlantic coastal lagoons (Figure 2a; Supporting Information Figure S13). Using the single value method for upland conversion, projections can result in similar mis-representations of future marsh area on the order of 10s of square kilometers (Figure 5a,b). Predictions of land conversion in the Chesapeake Bay region based on tidal datum (mean high water) alone suggest that 276 km^2 of uplands will convert to estuarine wetlands with 0.45 m of SLR and 968 km^2 of uplands will convert with 1.22 m of SLR (NOAA Office for Coastal Management, 2019). If brackish/transitional marsh is included (up to mean high water spring), the area increases to 778 km^2 and 1482 km^2 with 0.45 m and 1.22 m, respectively (NOAA Office for Coastal Management, 2019). These predictions do not allow currently developed or agricultural land to convert to marsh under any sea level rise scenario. Predictions which rely on threshold elevations determined independently of a tidal datum suggest that 962 and 1658 km^2 of uplands will convert with 0.45 m and 1.22 m of SLR (Molino et al., 2022), with impervious surfaces and agricultural land cover types removed (Chesapeake Conservancy, 2018). Deviations in predicted land conversion area within individual watersheds in some locations are in the opposite direction of regional predictions. For example, in North Landing River, one of the southernmost watersheds (HUC1 in Supporting Information Figure S1), 74 and 93 km^2 of uplands are predicted to convert to marsh under Low and Intermediate SLR scenarios by methods which rely on tidal datums (MHWS) (Figure 5, Table 2), while only 61 and 84 km^2 are

predicted to convert under similar SLR scenarios using spatially explicit threshold elevations (Figure 5, Table 2).

4 Discussion

4.1 Macro-scale drivers of threshold elevation

Strong gradients in tide range (0-1.21 m), salinity (<1-33 ppt), and other identified drivers of coastal treeline elevation make the Chesapeake Bay a dynamic system in which to apply the multiple linear regression model to understand macro-scale drivers of forest retreat (Figure 2). Our finding that threshold elevations increase with tidal range (Figure 3a) and that tidal range is the strongest predictor of threshold elevation in the multiple linear regression model (Table 1) supports the conceptual framework that tidal inundation is the dominant control on the lower bounds of the coastal treeline (Wasson et al., 2013; Williams et al., 1999). A similar relationship has been suggested for marshes across the coast of Mississippi in the Gulf of Mexico (Anderson et al., 2022). However, Mean High Water (MHW) only differs by 3.4 cm between tide gauges along the Mississippi coastline due to the regional geomorphic planform and hydrodynamics (Passeri et al., 2015), limiting the ability to test the effect of tidal range on threshold elevation across a broader range of conditions. Chesapeake Bay, as a large drowned river valley estuary, has greater variability in tide range and MHW along its coastal fringe and up tributaries, which facilitates assessment of this relationship. Indeed, machine learning applications have identified tidal variables as a key predictor of marsh migration area for all estuary types, including drowned river valleys, river estuaries, coastal bays, barrier estuaries, and intermittently closed and open lakes and lagoons (Hughes et al., 2022). The relationship between astronomical tidal range and threshold elevation is likely weakened by meteorological influences on tidal range. In microtidal

settings such as the Chesapeake Bay, wind has a significant impact on tides (Xiong & Berger, 2010), potentially increasing flooding frequency along marsh-forest boundaries in the lower tidal range portions of the region. As flood frequency can limit tree survival (Williams et al., 1999), we would expect this to influence the lower limit of coastal forests and weaken tide range as a variable.

Salinization of freshwater ecosystems is shifting species composition and limiting the extent of freshwater and terrestrial forests (Ensign & Noe, 2018; Noe et al., 2021; Taillie et al., 2019; Tully et al., 2019; E. White & Kaplan, 2017). Increases in salinity to coastal ecosystems commonly accompany increases in inundation from sea level rise (Williams et al., 1999), although salinization of tidal freshwater forests can independently affect tree mortality (Noe et al., 2021). Consistent with this conceptual framework, we find that threshold elevations increase with salinity (Figure 3b), and that salinity is a key driver of threshold in the multiple linear regression model (Table 1). Within the Atlantic coastal lagoon watersheds, which have the highest salinities in our study region (Figure 2a), exposure to highly saline waters from salt spray during storms measurably deviated the elevation of the coastal treeline from that expected by tidal range alone (Boon et al., 1977). In low salinity and low slope environments, representative of watersheds interspersed throughout our study region (Figure 2a,b), shading from plants has been shown to reduce evapotranspiration and facilitate forest regeneration, extending the lower limit of terrestrial forest, irrespective of increases in sea level rise and tidal inundation (Poulter et al., 2009; Veldkornet et al., 2015).

Regional slope has long been assumed to drive variability in lateral forest retreat rates, such that sea level rise inundates large areas and forest retreat rates are rapid in gently sloping regions (Brinson et al., 1995; Field et al., 2016; J. A. M. Smith, 2013). However, field evidence

supporting this relationship in Chesapeake Bay has been weak (Schieder et al., 2018) and in some cases it has been suggested that vertical migration rates are actually faster in high slope environments (Fagherazzi et al., 2019). Our finding that higher threshold elevations are found in higher slope environments therefore complicates the general assumption that forest retreat is fastest in low slope environments (Figure 4d, Table 1). There are several possible explanations for this finding. Steep slope environments are potentially more vulnerable to inundation because they have narrower transition zones from salt marsh to terrestrial forest, so that pulses of saltwater have a shorter distance to travel to reach freshwater ecosystems (Brinson et al., 1995; Fagherazzi et al., 2019). However, our model found no significant relationship between threshold elevation and distance to open water (Table 1). Higher slope environments are likely to have a greater outflow of fresh groundwater at the slope break, which occurs near the marsh-forest boundary (Brinson et al., 1995). While freshwater inputs would tend to reduce salinities and therefore potentially allow terrestrial vegetation to survive lower elevations (e.g. Figure 3b), regular saturation, even by freshwater, can stress terrestrial vegetation and deteriorate the soil organic matter (McDowell et al., 2022). Nevertheless, the unexpected positive relationship between threshold elevation and slope would benefit from further field investigations into the causal mechanisms at play.

Despite tidal range, salinity, and slope all having significant relationships with threshold elevation, the strength of these relationships was generally weak. It is possible that mild correlation between tidal range and salinity ($R^2 = 0.13$, $p < 0.01$) and average slope and salinity ($R^2 = 0.11$, $p < 0.01$) could be responsible. Tidal range and salinity tend to vary spatially with each other across the Chesapeake Bay region, where both salinity and tidal range are maximized at the mouth of the Bay and in the Atlantic coastal lagoons (Figure 2). Similarly, average slope

and salinity vary inversely with each other, despite differing reasons for these spatial trends (geomorphology vs proximity with the Atlantic Ocean) (Figure 2). Data resolution and quality also likely play a role in the weak model fit. For example, tidal range and salinity are both model outputs with low resolution (400-600 m; Table 1). Data for these variables do not exist at the marsh-forest boundary so the values used in the model are the median modeled values for each watershed.

Several previously established relationships between macro-scale environmental variables and forest mortality were found to be insignificant drivers of threshold elevation in our analysis. For example, storms act as a pulse disturbance that potentially results in rapid forest retreat (Fagherazzi et al., 2019; Miller et al., 2021; Ury et al., 2021). Hurricane Isabel, the largest named storm to affect the region since 1954, had storm surge reaching 2.4 m above highest astronomical tide in some areas of Chesapeake Bay and inundation which lasted for several days (Beven & Cobb, 2004). Hurricane Isabel likely resulted in a pulse of coastal forest retreat, at least in portions of the Chesapeake Bay near the Blackwater River, Maryland (Schieder & Kirwan, 2019). However, neither maximum depth of inundation nor inundation duration at the marsh-forest boundary was significantly correlated with threshold elevation in our analysis (Table 1). It remains unclear whether the storm impacts were short-lived and/or too localized to be relevant to the large spatial scales considered in our analysis, or whether the coarse resolution of the storm dataset (100-300 m) obscured trends. Further work is needed to quantify how flooding from repeated storm events might influence coastal forest retreat.

Our model also did not reveal a relationship between climate and threshold elevation, despite a variation of 3.6°C and 496 mm of rainfall throughout the Chesapeake region (Table 1). Temperature and precipitation are known to influence the growth rate of individual trees subject

to coastal flooding, and therefore their resilience to climate change and sea level rise (Desantis et al., 2007; Haaf et al., 2021; Kirwan et al., 2007). More work is needed to determine whether the insensitivity of threshold elevations to climatic in our analysis is real, or due to coarse data resolution.

4.2 Micro-scale drivers of threshold elevation

Interactions between local biotic and abiotic factors and global drivers can alter landscape-scale patterns in ecosystem transitions (Suding et al., 2015; Yando et al., 2018). Despite macro-scale drivers of threshold elevation (Figure 4, Table 1), the limited explanatory power of our linear model (44%) suggests that local drivers may additionally influence threshold elevation in ways that are not sufficiently captured in our large-scale analysis of the Chesapeake Bay region. Field observations suggest that tree species, hydrology, microtopography, and land use alter the expected threshold elevation from our model predictions (Figure 6).

Individual tree species response to local shifts in groundwater salinity and depth can alter coastal forest retreat irrespective of estuary-wide salinity trends (Gardner et al., 2002; Sacatelli et al., 2023; Thibodeau et al., 1998; Williams et al., 2007). The coastal forest in the Chesapeake Bay varies in composition from freshwater forested wetlands to loblolly pine forests to heterogeneous mixtures of pines and deciduous trees. Freshwater forested wetland species common to the southeastern U.S., such as bald cypress (*Taxodium distichum*), tend to be more tolerant to saturated soil conditions then terrestrial forests comprised of less flood tolerant species, such as red maple (*Acer rubrum*) (Kozlowski, 2002). Coastal tree species exist along a similar salinity gradient with coniferous trees, such as American holly (*Ilex opaca*) and eastern red cedar (*Juniperus virginiana*), considered to be more salt tolerant than deciduous trees (USDA NRCS Plant Materials Program, 2002b, 2002a). Younger age classes of both deciduous and

coniferous tree species are particularly susceptible to stress from salt and saturated soils. Red maple (*Acer rubrum*) seedlings experience reduced growth with saltwater flooding (Conner & Askew, 1993), while loblolly pine (*Pinus taeda*) experiences limited seedling recruitment in saturated soils (Kirwan et al., 2007). The ecological response of individual species based on unique flood and salt tolerances has the potential to hinder or accelerate the rate of coastal forest retreat across the estuary.

As sea level rises, the depth to groundwater and thickness of the unsaturated zone are predicted to decrease (Flemming et al., 2021), which may alter soil saturation and porewater salinity of the coastal zone. While high-resolution groundwater data does not yet exist on the scale of the Chesapeake Bay, we have observed indicator wetland species such as narrowleaf cattail (*Typha angustifolia*), commonly a sign of freshwater seepage (Silberhorn, 1999), along the marsh-forest boundary in one of our saltiest watersheds in the Atlantic coastal lagoons (Figure 2b), which illustrates a complex local hydrology (Figure 6b). Additional research is needed to scale up the relationship between individual tree species and groundwater dynamics to better capture the ecological response of coastal forests to sea level rise.

Microtopographic highs along the marsh-forest boundary can result in the presence of trees in areas that are below where terrestrial forests are predicted to occur. Trees in retreating coastal forests are commonly found on microtopographic highs such as the stumps or snags of dead trees (W. S. Kearney et al., 2019; Williams et al., 2007). These hummocks are high enough above regular inundation that seedlings of terrestrial tree species can germinate and grow (Figure 6c) and freshwater input from rainfall maintains healthier root zones compared to the anoxic soils of hollows (Krauss et al., 2023). Digital elevation models, even at high resolutions of 1 m (Danielson & Tyler, 2016), are likely not able to capture these local topographic highs, resulting

in the threshold elevations that more closely reflect the lower elevation areas where marsh vegetation is present.

Roads, ditches, and levees constructed in the coastal plain can artificially alter the apparent elevation of transition between marsh and upland ecosystems. In the Chesapeake Bay, small earthen levees at the boundary between marsh and upland reduce tidal inundation of agricultural and private lands (Hall et al., 2022; Putalik & Davis, 2022). These earthen levees can have large trees growing on them (Figure 6a) making it difficult to discern between a natural marsh-forest boundary and a forested levee with anomalously high threshold elevations. No dataset of privately-owned levees exists for the Chesapeake region, making it difficult to identify threshold elevation points which fall on these features. Together, these local drivers make it difficult to quantify threshold elevations, and limit our ability to predict future marsh migration into retreating terrestrial ecosystems.

4.3 Implications for projections of future marsh migration area

Quantifying the drivers of shifting ecotones is a critical step for predicting the impacts of sea level rise on future land use change. For example, most projections of future marsh area rely on selecting a tidal datum that defines the current landward boundary of marsh extent (Holmquist et al., 2021; Mitchell et al., 2020), or selecting a tidal datum as the future boundary of marsh extent (Buchanan et al., 2022; Osland et al., 2022; Warnell et al., 2022). However, our results demonstrate that the elevation of transition (i.e., threshold elevation in m NAVD88) between marsh and forest varies substantially with salinity, slope, and local drivers. Where a single value, such as HAT, or MHHWS are used to dictate the current landward extent of salt marshes (Holmquist et al., 2021; Mitchell et al., 2020), the resulting threshold elevations can differ from our measured threshold elevations by 0.29-0.44 m (Table 2). This difference is similar to or

exceeds the magnitude of projected sea level rise in Chesapeake Bay by 2050 (Sweet et al., 2017) and suggests that projections which use tidal datums as a proxy for threshold elevations miss the majority of variability. As a result, future marsh area projections made using a single value for threshold elevation across watersheds with different topographies and salinities can vary widely from projections made using spatially explicit delineations of the marsh-forest boundary (Figure 5a,b). For example, in watersheds with low salinities and corresponding low threshold elevations, projected marsh migration areas can be underestimated by 200-400% when a single threshold elevation is applied regionally (Table 2).

Our results also differ from studies which rely solely on tidal datums, where future salt marsh extent is dictated by the location and elevation of future Mean High Water (MHW) and the limit of brackish/transitional marsh is dictated by future mean high water spring (MHWS) (NOAA Office for Coastal Management, 2019). As discussed previously, actual threshold elevations are highly variable in Chesapeake Bay and cannot be described solely through tidal datums. Projections of future marsh migration area under the Low SLR Scenario (0.45 m) made using our spatially explicit approach (962 km^2; Molino et al. 2022) are similar to those using future MHWS as the landward extent of marsh (778 km^2; NOAA Office of Coastal Management 2019). We attribute differences in marsh migration area estimates between methods at a watershed-scale largely to variation in macro-scale drivers. In high salinity watersheds, such as the Virginia Atlantic coastal lagoons, projections based on tidal datums alone tend to underestimate marsh migration area (Table 2). In low salinity watersheds, such as North Landing River, Virginia, projections based on tidal datums alone tend to overestimate marsh migration area (Figure 5b,c). Nevertheless, differences in projected marsh migration area under alternative methods lessen under higher SLR scenarios (Table 2). Rates of relative sea level rise and

planning timelines for decision-making are essential considerations when selecting a projection method (Gesch, 2012), with the spatially explicit approach providing additional insight on shorter timespans and lower SLR scenarios.

The physical and climatic drivers which are used to predict ecosystem change also have uncertain future trends. Global climate models predict increases and decreases in future annual precipitation which will have a strong influence on estuarine salinity gradients. Similarly, tidal range may vary in the future based on changes in mean sea level and shoreline hardening (Blyth Lee et al., 2017; Cai et al., 2022), which is further complicated by shifts in storminess that cause barrier islands to form and breach, limiting or increasing tidal flushing (Yellen et al., 2023). Our work demonstrates a path forward to incorporating these complex and dynamic changes into future predictions of land use change by utilizing independently established ecosystem boundaries rather than static tidal datums. This approach is particularly important along spatially variable coastlines such as the North American Atlantic seaboard where limited resources are being split between flood adaptation and defense measures. With global marshes predicted to struggle to keep pace with SLR in the vertical dimension (Saintilan et al., 2022), lateral migration is becoming a dominant large-scale conservation option. Conservation efforts may be implemented at regional or local levels (Coastal Protection and Restoration Authority of Louisiana, 2017; Millard et al., 2013). Therefore, local-regional predictions based on higher resolution input datasets (Van Coppenolle & Temmerman, 2020; Enwright et al., 2016) are needed to inform management of coastal ecosystems and ensure maintenance of global marsh area into the coming decades.

5 Conclusions

Global processes, such as sea level rise, are responsible for landscape-scale shifts in coastal ecosystems extent (Hein & Kirwan, In press; A. J. Smith & Goetz, 2021; E. White & Kaplan, 2017). We found that within the Chesapeake Bay, tidal range, salinity, and slope are macro-scale drivers of coastal forest conversion to marsh. The importance of tidal inundation and salinity as abiotic controls on the lower limit of coastal forest is well supported (J. A. M. Smith, 2013; Veldkornet et al., 2015; Williams et al., 1999), while the positive relationship between slope and threshold elevation suggests more complex underlying dynamics at play. However, the combined influence of these macro-scale drivers explains less than half of the regional variability in threshold elevation. This unexplained variability suggests that micro-scale drivers, such as hydrology, microtopography, and infrastructure, are also strong controls on the location of the marsh-forest boundary. Thus, our work finds that conventional methods that rely on tidal datums to predict the marsh-forest boundary may produce projections that over- or under-estimate future marsh migration areas.

Acknowledgments

This work was funded by the U.S. Geological Survey Climate Research and Development and the U.S. Geological Survey Coastal and Marine Hazards and Resources Program. Additional funding was provided from the National Science Foundation CAREER, LTER, and CZN programs (EAR-1654374, DEB-1832221, and EAR-2012670). We would like to thank Marjy Friedrichs and Pierre St-Laurent for providing the salinity model output, Yaping Chen for curating the climate datasets, and Alfredo Aretxabaleta for navigating the ADCIRC Prediction System to provide the Hurricane Isabel product used in this study. Any use of trade, firm, or

519 product names is for descriptive purposes only and does not imply endorsement by the U.S.
520 Government.
521
522 **Open Research**
523 **Data Availability Statement**
524 Threshold elevation data is available in the Environmental Data Initiative repository (Molino,
525 Carr, et al., 2021). Watershed-scale dataset containing all 14 variables used in the linear model
526 can be found in Table 1 in Supporting Information and in the Environmental Data Initiative
527 repository (Molino et al., 2023). Python script used to run the linear model is published in the
528 Environmental Data Initiative repository (Molino et al., 2023). Original dataset sources and link
529 to the data are compiled in Table 1 and cited in-text (Methods 2.2 Input variables). Marsh
530 migration projections are available through the NOAA Sea Level Rise Viewer [dataset]
531 (https://coast.noaa.gov/slr/). Linear model was run using open source software (Python 3
532 [software], https://www.python.org/) and statistical modeling package (statsmodel 0.14.0
533 [software], https://www.statsmodels.org/stable/index.html).
534
535 **References**
536 Anderson, C. P., Carter, G. A., & Waldron, M. C. B. (2022). Precise Elevation Thresholds
537 Associated with Salt Marsh–Upland Ecotones along the Mississippi Gulf Coast. *Annals of*
538 *the American Association of Geographers*. https://doi.org/10.1080/24694452.2022.2047593
539 Beven, J., & Cobb, H. (2004). *Tropical Cyclone Report: Hurricane Isabel*. Retrieved from
540 https://www.nhc.noaa.gov/data/tcr/AL132003_Isabel.pdf
541 Blyth Lee, S., Li, M., & Zhang, F. (2017). Impact of sea level rise on tidal range in Chesapeake

and Delaware Bays. *Journal of Geophyscial Research: Oceans*, *122*, 3917–3938. https://doi.org/10.1002/2016JC012597

Boon, J. D., Boule, M. E., & Silberhorn, G. M. (1977). Delineation of Tidal Boundaries in Lower Chesapeake Bay and its Tributaries. *Special Reports in Applied Marine Science and Ocean Engineering (SRAMSOE)*, (No. 140). https://doi.org/10.21220/V50160

Brinson, M. M., Christian, R. R., & Blum, L. K. (1995). Multiple States in the Sea-Level Induced Transition from Terrestrial Forest to Estuary. *Estuaries*, *18*(4), 648–659. Retrieved from https://www.jstor.org/stable/1352383

Brittain, R. A., & Craft, C. B. (2012). Effects of sea-level rise and anthropogenic development on priority bird species habitats in coastal Georgia, USA. *Environmental Management*, *49*, 473–482. https://doi.org/10.1007/s00267-011-9761-x

Buchanan, M. K., Kulp, S., & Strauss, B. (2022). Resilience of U.S. coastal wetlands to accelerating sea level rise. *Environmental Research Communications*, *4*. https://doi.org/10.1088/2515-7620/ac6eef

Cai, X., Qin, Q., Shen, J., & Zhang, Y. J. (2022). Bifurcate responses of tidal range to sea-level rise in estuaries with marsh evolution. *Limnology and Oceanography Letters*, *7*(3), 210–217. https://doi.org/10.1002/lol2.10256

Chen, Y., & Kirwan, M. L. (2022a). A phenology- and trend-based approach for accurate mapping of sea-level driven coastal forest retreat. *Remote Sensing of the Environment*, *281*(113229). https://doi.org/10.1016/j.rse.2022.113229

Chen, Y., & Kirwan, M. L. (2022b). Climate-driven decoupling of wetland and upland biomass trends on the mid-Atlantic coast. *Nature Geoscience*, *15*(11), 913–918. https://doi.org/10.1038/s41561-022-01041-x

565 Chesapeake Conservancy. (2018). Land Use Data Project 2013/2014. [dataset]. Retrieved
566 September 6, 2019, from https://chesapeakeconservancy.org/conservation-innovation-
567 center/high-resolution-data/land-use-data-project/
568 Coastal Protection and Restoration Authority of Louisiana. (2017). *Louisiana's Comprehensive*
569 *Master Plan for a Sustainable Coast*. Baton Rouge. Retrieved from http://coastal.la.gov/wp-
570 content/uploads/2017/04/2017-Coastal-Master-Plan_Web-Book_CFinal-with-Effective-
571 Date-06092017.pdf
572 Conner, W. H., & Askew, G. R. (1993). Impact of Saltwater Flooding on Red Maple, Redbay,
573 and Chinese Tallow Seedlings. *Southern Appalachian Botanical Society*, *58*(3), 214–219.
574 https://doi.org/https://www.jstor.org/stable/4033645
575 Van Coppenolle, R., & Temmerman, S. (2020). Identifying Ecosystem Surface Areas Available
576 for Nature-Based Flood Risk Mitigation in Coastal Cities Around the World. *Estuaries and*
577 *Coasts*, *43*, 1335–1344. https://doi.org/10.1007/s12237-020-00718-z
578 Craft, C., Clough, J., Ehman, J., Jove, S., Park, R., Pennings, S., et al. (2009). Forecasting the
579 effects of accelerated sea-level rise on tidal marsh ecosystem services. *Frontiers in Ecology*
580 *and the Environment*, *7*(2), 73–78. https://doi.org/10.1890/070219
581 Danielson, J., & Tyler, D. (2016). Topobathymetric Model for Chesapeake Bay Region - District
582 of Columbia, States of Delaware, Maryland, Pennsylvania, and Virginia, 1859 to 2015.
583 [dataset]. Retrieved January 29, 2020, from
584 https://topotools.cr.usgs.gov/topobathy_viewer/dwndata.htm
585 Desantis, L. R. G., Bhotika, S., Williams, K., & Putz, F. E. (2007). Sea-level rise and drought
586 interactions accelerate forest decline on the Gulf Coast of Florida, USA. *Global Change*
587 *Biology*, *13*(11), 2349–2360. https://doi.org/10.1111/j.1365-2486.2007.01440.x

588 Doyle, T. W., Krauss, K. W., Conner, W. H., & From, A. S. (2010). Predicting the retreat and
589 migration of tidal forests along the northern Gulf of Mexico under sea-level rise. *Forest*
590 *Ecology and Management*, *259*(4), 770–777. https://doi.org/10.1016/j.foreco.2009.10.023
591 Duran Vinent, O., Herbert, E. R., Coleman, D. J., Himmelstein, J. D., & Kirwan, M. L. (2021).
592 Onset of runaway fragmentation of salt marshes. *One Earth*, *4*, 506–516.
593 https://doi.org/10.1016/j.oneear.2021.02.013
594 Ensign, S. H., & Noe, G. B. (2018). Tidal extension and sea-level rise: recommendations for a
595 research agenda. *Frontiers in Ecology and the Environment*, *16*(1), 37–43.
596 https://doi.org/10.1002/fee.1745
597 Enwright, N. M., Griffith, K. T., & Osland, M. J. (2016). Barriers to and opportunities for
598 landward migration of coastal wetlands with sea-level rise. *Frontiers in Ecology and the*
599 *Environment*, *14*(6), 307–316. https://doi.org/10.1002/fee.1282
600 Ezer, T. (2023). Sea level acceleration and variability in the Chesapeake Bay: past trends, future
601 projections, and spatial variations within the Bay. *Ocean Dynamics*, *73*(1), 23–34.
602 https://doi.org/10.1007/s10236-022-01536-6
603 Ezer, T., & Atkinson, L. P. (2015). Sea Level Rise in Virginia – Causes, Effects and Response.
604 *Virginia Journal of Science*, *66*(3). https://doi.org/10.25778/8w61-qe76
605 Fagherazzi, S., Anisfeld, S. C., Blum, L. K., Long, E. V., Feagin, R. A., Fernandes, A., et al.
606 (2019). Sea level rise and the dynamics of the marsh-upland boundary. *Frontiers in*
607 *Environmental Science*, *7*(25). https://doi.org/10.3389/fenvs.2019.00025
608 Field, C. R., Gjerdrum, C., & Elphick, C. S. (2016). Forest resistance to sea-level rise prevents
609 landward migration of tidal marsh. *Biological Conservation*, *201*, 363–369.
610 https://doi.org/10.1016/j.biocon.2016.07.035

611 Flemming, B. J., Raffensperger, J., Goodling, P. J., & Masterson, J. P. (2021). *Simulated Effects*
612 *of Sea-Level Rise on the Shallow, Fresh Groundwater System of Assateague Island,*
613 *Maryland and Virginia: U.S. Geological Survey Scientific Investigations Report 2020–*
614 *5104*. Reston, Virginia. https://doi.org/10.3133/sir20205104.
615 Gardner, L. R., Reeves, H. W., & Thibodeau, P. M. (2002). Groundwater dynamics along forest-
616 marsh transects in a southeastern salt marsh, USA: Description, interpretation and
617 challenges for numerical modeling. *Wetlands Ecology and Management*, *10*, 145–159.
618 Gesch, D. B. (2012). Elevation Uncertainty in Coastal Inundation Hazard Assessments. In S.
619 Cheval (Ed.), *Natural Disasters* (pp. 121–140). InTech. https://doi.org/10.5772/31972
620 Guimond, J. A., & Michael, H. A. (2021). Effects of Marsh Migration on Flooding, Saltwater
621 Intrusion, and Crop Yield in Coastal Agricultural Land Subject to Storm Surge Inundation.
622 *Water Resources Research*, *57*. https://doi.org/10.1029/2020WR028326
623 Guimond, J. A., Yu, X., Seyfferth, A. L., & Michael, H. A. (2020). Using Hydrological-
624 Biogeochemical Linkages to Elucidate Carbon Dynamics in Coastal Marshes Subject to
625 Relative Sea Level Rise. *Water Resources Research*, *56*.
626 https://doi.org/10.1029/2019WR026302
627 Haaf, L., Dymond, S. F., & Kreeger, D. A. (2021). Principal Factors Influencing Tree Growth in
628 Low-Lying Mid Atlantic Coastal Forests. *Forests*, *12*(10), 1351.
629 https://doi.org/10.3390/f12101351
630 Hall, E. A., Molino, G. D., Messerschmidt, T., & Kirwan, M. L. (2022). Hidden levees: Small-
631 scale flood defense on rural coasts. *Anthropocene*, *40*(100350).
632 https://doi.org/10.1016/j.ancene.2022.100350
633 Hein, C. J., & Kirwan, M. L. (2024). Marine Transgression in Modern Times. *Annual Review of*

Marine Science, *16*. https://doi.org/10.1146/annurev-marine-022123-103802

Holmquist, J. R., Windham-Myers, L., Bernal, B., Byrd, K., Crooks, S., Gonneea, M., et al. (2019). *Coastal Wetland Elevation and Carbon Flux Inventory with Uncertainty, USA, 2006-2011*. Oak Ridge, Tennessee, USA. [dataset]. https://doi.org/10.3334/ORNLDAAC/1650

Holmquist, J. R., Brown, L. N., & MacDonald, G. M. (2021). Localized Scenarios and Latitudinal Patterns of Vertical and Lateral Resilience of Tidal Marshes to Sea-Level Rise in the Contiguous United States. *Earth's Future*, *9*(6). https://doi.org/10.1029/2020ef001804

Hughes, M. G., Glasby, T. M., Hanslow, D. J., West, G. J., & Wen, L. (2022). Random Forest Classification Method for Predicting Intertidal Wetland Migration Under Sea Level Rise. *Frontiers in Environmental Science*, *10*. https://doi.org/10.3389/fenvs.2022.749950

Hussein, A. H. (2009). Modeling of Sea-Level Rise and Deforestation in Submerging Coastal Ultisols of Chesapeake Bay. *Soil Science Society of America Journal*, *73*(1), 185–196. https://doi.org/10.2136/sssaj2006.0436

Hussein, A. H., & Rabenhorst, M. C. (2001). Tidal Inundation of Transgressive Coastal Areas. *Soil Science Society of America Journal*, *65*, 536–544. https://doi.org/10.2136/sssaj2001.652536x

Jobe IV, J. G. D., & Gedan, K. (2021). Species-specific responses of a marsh-forest ecotone plant community responding to climate change. *Ecology*, *102*(4). https://doi.org/10.1002/ecy.3296

Kearney, M. S., Rogers, A. S., Townshend, J. R. G., Rizzo, E., Stutzer, D., Stevenson, J. C., & Sundborg, K. (2002). Landsat Imagery Shows Decline of Coastal Marshes in Chesapeake

and Delaware Bays. *Eos*, *83*(16), 173–184. https://doi.org/10.1029/2002EO000112

Kearney, W. S., Fernandes, A., & Fagherazzi, S. (2019). Sea-level rise and storm surges structure coastal forests into persistence and regeneration niches. *PLoS ONE*, *14*(5). https://doi.org/10.1371/journal.pone.0215977

Kirwan, M. L., Kirwan, J. L., & Copenheaver, C. A. (2007). Dynamics of an Estuarine Forest and its Response to Rising Sea Level. *Journal of Coastal Research*, *23*(2), 457–463. https://doi.org/10.2112/04-0211.1

Kirwan, M. L., Walters, D. C., Reay, W. G., & Carr, J. A. (2016). Sea level driven marsh expansion in a coupled model of marsh erosion and migration. *Geophysical Research Letters*, *43*(9), 4366–4373. https://doi.org/10.1002/2016GL068507

Kozlowski, T. T. (2002). Physiological-ecological impacts of flooding on riparian forest ecosystems. *Wetlands*, *22*(3), 550–561. https://doi.org/10.1672/0277-5212(2002)022[0550:PEIOFO]2.0.CO;2

Krauss, K. W., Noe, G. B., Duberstein, J. A., Cormier, N., From, A. S., Doody, T. R., et al. (2023). Presence of Hummock and Hollow Microtopography Reflects Shifting Balances of Shallow Subsidence and Root Zone Expansion Along Forested Wetland River Gradients. *Estuaries and Coasts*. https://doi.org/10.1007/s12237-023-01227-5

Langston, A. K., Coleman, D. J., Jung, N. W., Shawler, J. L., Smith, A. J., Williams, B. L., et al. (2021). The Effect of Marsh Age on Ecosystem Function in a Rapidly Transgressing Marsh. *Ecosystems*. https://doi.org/10.1007/s10021-021-00652-6

McDowell, N. G., Ball, M., Bond-Lamberty, B., Kirwan, M. L., Krauss, K. W., Megonigal, J. P., et al. (2022). Processes and mechanisms of coastal woody-plant mortality. *Global Change Biology*, *28*(20), 5881–5900. https://doi.org/10.1111/gcb.16297

Messerschmidt, T. C., Langston, A. K., & Kirwan, M. L. (2021). Asymmetric root distributions reveal press–pulse responses in retreating coastal forests. *Ecology*, *102*(10), 1–7. https://doi.org/10.1002/ecy.3468

Millard, K., Redden, A. M., Webster, T., & Stewart, H. (2013). Use of GIS and high resolution LiDAR in salt marsh restoration site suitability assessments in the upper Bay of Fundy, Canada. *Wetlands Ecology and Management*, *21*, 243–262. https://doi.org/10.1007/s11273-013-9303-9

Miller, C. B., Rodriguez, A. B., & Bost, M. C. (2021). Sea-level rise, localized subsidence, and increased storminess promote saltmarsh transgression across low-gradient upland areas. *Quaternary Science Reviews*, *265*. https://doi.org/10.1016/j.quascirev.2021.107000

Mitchell, M., Herman, J., & Hershner, C. (2020). Evolution of Tidal Marsh Distribution under Accelerating Sea Level Rise. *Wetlands*, *40*(6), 1789–1800. https://doi.org/10.1007/s13157-020-01387-1

Molino, G. D., Defne, Z., Ganju, N. K., Carr, J. A., Gutenspergen, G. R., & Walters, D. C. (2020). Slope Values Across Marsh-Forest Boundary in Chesapeake Bay Region, USA. [dataset]. https://doi.org/10.5066/P9EJ6PGT

Molino, G. D., Carr, J. A., Ganju, N. K., & Kirwan, M. L. (2021). Data Repository for Spatial Variability in Marsh Vulnerability and Coastal Forest Loss in Chesapeake Bay ver. 2. Environmental Data Initiative. [dataset]. https://doi.org/10.6073/pasta/d57c49f666bd8b7ad692a5230573e020

Molino, G. D., Defne, Z., Aretxabaleta, A. L., Ganju, N. K., & Carr, J. A. (2021). Quantifying Slopes as a Driver of Forest to Marsh Conversion Using Geospatial Techniques: Application to Chesapeake Bay Coastal-Plain, United States. *Frontiers in Environmental*

Science, *9*. https://doi.org/10.3389/fenvs.2021.616319

Molino, G. D., Carr, J. A., Ganju, N. K., & Kirwan, M. L. (2022). Variability in marsh migration potential determined by topographic rather than anthropogenic constraints in the Chesapeake Bay region. *Limnology and Oceanography Letters*, *7*(4). https://doi.org/10.1002/lol2.10262

Molino, G. D., Carr, J. A., Ganju, N. K., & Kirwan, M. L. (2023). Characteristics of the Marsh-Forest Boundary within Chesapeake Bay Region Coastal Watersheds. [dataset]. https://doi.org/10.6073/pasta/9866ba31b6ee10ade8de22a54a305b6d

NOAA Office for Coastal Management. (2019). Marsh Migration. Charleston, SC: InPort. [dataset]. Retrieved from https://www.fisheries.noaa.gov/inport/item/55958

Noe, G. B., Cashman, M. J., Skalak, K., Gellis, A., Hopkins, K. G., Moyer, D., et al. (2020). Sediment dynamics and implications for management: State of the science from long-term research in the Chesapeake Bay watershed, USA. *WIREs Water*, *7:e1454*. https://doi.org/10.1002/wat2.1454

Noe, G. B., Bourg, N. A., Krauss, K. W., Duberstein, J. A., & Hupp, C. R. (2021). Watershed and Estuarine Controls Both Influence Plant Community and Tree Growth Changes in Tidal Freshwater Forested Wetlands along Two U.S. Mid-Atlantic Rivers. *Forests*, *12*(9). https://doi.org/10.3390/f12091182

Nordio, G., Frederiks, R., Hingst, M., Carr, J., Kirwan, M., Gedan, K., et al. (2023). Frequent Storm Surges Affect the Groundwater of Coastal Ecosystems. *Geophysical Research Letters*, *50*. https://doi.org/10.1029/2022GL100191

Oertel, G. F. (1985). The barrier island system. *Marine Geology*, *63*(1–4), 1–18. https://doi.org/10.1016/0025-3227(85)90077-5

726 Osland, M. J., Chivoiu, B., Enwright, N. M., Thorne, K. M., Guntenspergen, G. R., Grace, J. B.,
727 et al. (2022). Migration and transformation of coastal wetlands in response to rising seas.
728 *Science Advances*, *8*(26). https://doi.org/10.1126/sciadv.abo5174
729 Passeri, D. L., Hagen, S. C., Medeiros, S. C., & Bilskie, M. V. (2015). Impacts of historic
730 morphology and sea level rise on tidal hydrodynamics in a microtidal estuary (Grand Bay,
731 Mississippi). *Continental Shelf Research*, *111*, 150–158.
732 https://doi.org/10.1016/j.csr.2015.08.001
733 Pekel, J.-F., Cottam, A., Gorelick, N., & Belward, A. S. (2016). High-resolution mapping of
734 global surface water and its long-term changes. *Nature*, *540*, 418–422.
735 https://doi.org/10.1038/nature20584
736 Perry, J. E., Barnard, T. A., Bradshaw, J. G., Friedrichs, C. T., Havens, K. J., Mason, P. A., et al.
737 (2001). Creating Tidal Salt Marshes in the Chesapeake Bay. *Journal of Coastal Research*,
738 (27), 170–191. Retrieved from https://www.jstor.org/stable/25736172
739 Poulter, B., Qian, S. S., & Christensen, N. L. (2009). Determinants of coastal treeline and the
740 role of abiotic and biotic interactions. *Plant Ecology*, *202*, 55–66.
741 https://doi.org/10.1007/s11258-008-9465-3
742 PRISM Climate Group Oregon State University. (2019). PRISM Gridded Climate Data.
743 [dataset]. Retrieved July 7, 2021, from https://prism.oregonstate.edu
744 Putalik, E., & Davis, B. (2022). Bay Migrations. Retrieved October 25, 2022, from
745 https://placesjournal.org/article/climate-and-migration-in-the-chesapeake-marsh/?cn-
746 reloaded=1&cn-reloaded=1#0
747 Robichaud, A., & Begin, Y. (1997). The Effects of Storms and Sea-Level Rise on a Coastal
748 Forest Margin in New Brunswick, Eastern Canada. *Journal of Coastal Research*, *13*(2),

429–439. Retrieved from https://www.jstor.org/stable/4298638

Sacatelli, R., Kaplan, M., Carleton, G., & Lathrop, R. G. (2023). Coastal Forest Dieback in the Northeast USA: Potential Mechanisms and Management Responses. *Sustainability*, *15*(6346). https://doi.org/10.3390/su15086346

Saintilan, N., Kovalenko, K. E., Guntenspergen, G., Rogers, K., Lynch, J. C., Cahoon, D. R., et al. (2022). Constraints on the adjustment of tidal marshes to accelerating sea level rise. *Science*, *377*(6605), 523–527. https://doi.org/10.1126/science.abo7872

Schieder, N. W., & Kirwan, M. L. (2019). Sea-level driven acceleration in coastal forest retreat. *Geology*, *47*(12), 1151–1155. https://doi.org/10.1130/G46607.1

Schieder, N. W., Walters, D. C., & Kirwan, M. L. (2018). Massive Upland to Wetland Conversion Compensated for Historical Marsh Loss in Chesapeake Bay, USA. *Estuaries and Coasts*, *41*, 940–951. https://doi.org/10.1007/s12237-017-0336-9

Schuerch, M., Spencer, T., Temmerman, S., Kirwan, M. L., Wolff, C., Lincke, D., et al. (2018). Future response of global coastal wetlands to sea-level rise. *Nature*, *561*(7722), 231–234. https://doi.org/10.1038/s41586-018-0476-5

Shaw, P., Jobe, J., & Gedan, K. B. (2022). Environmental Limits on the Spread of Invasive Phragmites australis into Upland Forests with Marine Transgression. *Estuaries and Coasts*, *45*(2), 539–550. https://doi.org/10.1007/s12237-021-00980-9

Silberhorn, G. M. (1999). *Common Plants of the Mid-Atlantic Coast: A Field Guide* (Revised). Baltimore: The Johns Hopkins University Press.

Smith, A. J., & Goetz, E. M. (2021). Climate change drives increased directional movement of landscape ecotones. *Landscape Ecology*. https://doi.org/10.1007/s10980-021-01314-7

Smith, A. J., & Kirwan, M. L. (2021). Sea Level-Driven Marsh Migration Results in Rapid Net

772 Loss of Carbon. *Geophysical Research Letters*, *48*. https://doi.org/10.1029/2021GL092420
773 Smith, J. A. M. (2013). The Role of Phragmites australis in Mediating Inland Salt Marsh
774 Migration in a Mid-Atlantic Estuary. *PLoS ONE*, *8*(5).
775 https://doi.org/10.1371/journal.pone.0065091
776 Suding, K. N., Farrer, E. C., King, A. J., Kueppers, L., & Spasojevic, M. J. (2015). Vegetation
777 change at high elevation: scale dependence and interactive effects on Niwot Ridge. *Plant*
778 *Ecology and Diversity*, *8*(5–6), 713–725. https://doi.org/10.1080/17550874.2015.1010189
779 Sweet, W. V., Kopp, R. E., Weaver, C. P., Obeysekera, J., Horton, R. M., Thieler, E. R., &
780 Zervas, C. (2017). Global and Regional Sea Level Rise Scenarios for the United States.
781 NOAA Technical Report NOS CO-OP 83. [dataset]. Retrieved from
782 https://tidesandcurrents.noaa.gov/publications/techrpt83_Global_and_Regional_SLR_Scena
783 rios_for_the_US_final.pdf
784 Taillie, P. J., Moorman, C. E., Poulter, B., Ardón, M., & Emanuel, R. E. (2019). Decadal-Scale
785 Vegetation Change Driven by Salinity at Leading Edge of Rising Sea Level. *Ecosystems*,
786 *22*(8), 1918–1930. https://doi.org/10.1007/s10021-019-00382-w
787 Thibodeau, P. M., Gardner, L. R., & Reeves, H. W. (1998). The role of groundwater flow in
788 controlling the spatial distribution of soil salinity and rooted macrophytes in a southeastern
789 salt marsh, USA. *Mangroves and Salt Marshes*, *2*, 1–13.
790 https://doi.org/10.1023/A:1009910712539
791 Tully, K., Gedan, K., Epanchin-Niell, R., Strong, A., Bernhardt, E. S., Bendor, T., et al. (2019).
792 The Invisible Flood: The Chemistry, Ecology, and Social Implications of Coastal Saltwater
793 Intrusion. *BioScience*, *69*(5), 368–378. https://doi.org/10.1093/biosci/biz027
794 U.S. Fish and Wildlife Service. (2018). *National Wetlands Inventory: Wetlands Mapper*. U.S.

795 Department of the Interior, Fish and Wildlife Service, Washington, D.C. [dataset].
796 Retrieved from https://www.fws.gov/wetlands/
797 Ury, E. A., Yang, X., Wright, J. P., & Bernhardt, E. S. (2021). Rapid deforestation of a coastal
798 landscape driven by sea-level rise and extreme events. *Ecological Applications*, *31*(5).
799 https://doi.org/10.1002/eap.2339
800 USDA NRCS Plant Materials Program. (2002a). Plant Fact Sheet: American Holly. Retrieved
801 July 18, 2023, from https://plants.usda.gov/DocumentLibrary/factsheet/pdf/fs_ilop.pdf
802 USDA NRCS Plant Materials Program. (2002b). Plant Fact Sheet: Eastern Red Cedar. Retrieved
803 July 18, 2023, from https://plants.usda.gov/DocumentLibrary/factsheet/pdf/fs_juvi.pdf
804 USGS. (2020). USGS Watershed Boundary Dataset (WBD) for 2-digit Hydrologic Unit - 02
805 (published 20201203). *ScienceBase*. U.S. Geological Survey (USGS). [dataset]. Retrieved
806 from https://www.sciencebase.gov/catalog/item/5a1632b2e4b09fc93dd171d9
807 Veldkornet, D. A., Adams, J. B., & Potts, A. J. (2015). Where do you draw the line?
808 Determining the transition thresholds between estuarine salt marshes and terrestrial
809 vegetation. *South African Journal of Botany*, *101*, 153–159.
810 https://doi.org/10.1016/j.sajb.2015.05.003
811 Warnell, K., Olander, L., & Currin, C. (2022). Sea level rise drives carbon and habitat loss in the
812 U.S. mid-Atlantic coastal zone. *PLOS Climate*, *1*(6).
813 https://doi.org/10.1371/journal.pclm.0000044
814 Wasson, K., Woolfolk, A., & Fresquez, C. (2013). Ecotones as Indicators of Changing
815 Environmental Conditions: Rapid Migration of Salt Marsh–Upland Boundaries. *Estuaries*
816 *and Coasts*, *36*, 654–664. https://doi.org/10.1007/s12237-013-9601-8
817 White, E., & Kaplan, D. (2017). Restore or retreat? Saltwater intrusion and water management in

818 coastal wetlands. *Ecosystem Health and Sustainability*, *3*(1).
819 https://doi.org/10.1002/ehs2.1258
820 White, E. E., Ury, E. A., Bernhardt, E. S., & Yang, X. (2021). Climate Change Driving
821 Widespread Loss of Coastal Forested Wetlands Throughout the North American Coastal
822 Plain. *Ecosystems*. https://doi.org/10.1007/s10021-021-00686-w
823 Williams, K., Ewel, K. C., Stumpf, R. P., Putz, F. E., Workman, T. W., Williams, K., et al.
824 (1999). Sea-Level Rise and Coastal Forest Retreat on the West Coast of Florida, USA.
825 *Ecology*, *80*(6), 2045–2063. Retrieved from https://www.jstor.org/stable/176677
826 Williams, K., MacDonald, M., & McPherson, K. (2007). Chapter 10 - Ecology of the Coastal
827 Edge of Hydric Hammocks on the Gulf Coast of Florida. In W. H. Conner, T. W. Doyle, &
828 K. W. Krauss (Eds.), *Ecology of Tidal Freshwater Forested Wetlands of the Southeastern*
829 *United States* (pp. 255–289). Springer.
830 Xiong, Y., & Berger, C. R. (2010). Chesapeake Bay Tidal Characteristics. *Journal of Water*
831 *Resource and Protection*, *2*, 619–628. https://doi.org/10.4236/jwarp.2010.27071
832 Yando, E. S., Osland, M. J., & Hester, M. W. (2018). Microspatial ecotone dynamics at a
833 shifting range limit: plant–soil variation across salt marsh–mangrove interfaces. *Oecologia*,
834 *187*, 319–331. https://doi.org/10.1007/s00442-018-4098-2
835 Yellen, B., Woodruff, J. D., Baranes, H. E., Engelhart, S. E., Geywer, W. R., Randall, N., &
836 Griswold, F. R. (2023). Salt Marsh Response to Inlet Switch-Induced Increases in Tidal
837 Inundation. *Journal of Geophysical Research: Earth Surface*, *128*.
838 https://doi.org/10.1029/2022jf006815
839 Zinnert, J. C., Via, S. M., Nettleton, B. P., Tuley, P. A., Moore, L. J., & Stallins, J. A. (2019).
840 Connectivity in coastal systems: Barrier island vegetation influences upland migration in a

changing climate. *Global Change Biology*, *25*(7), 2419–2430. https://doi.org/10.1111/gcb.14635

Zuur, A. F., Ieno, E. N., Walker, N., Saveliev, A. A., & Smith, G. M. (2009). *Mixed effects models and extensions in ecology with R* (1st ed.). New York, NY: Springer. https://doi.org/10.1007/978-0-387-87458-6

Tables and Figure Captions

Figure 1. a-b) Example of a marsh-forest boundary on a York River tributary, Virginia. a) Forest extent determined from the Chesapeake Conservancy High-Resolution Land Use Data Project "forest" classification (Chesapeake Conservancy, 2018). Salt marsh extent obtained from Maryland and Virginia National Wetlands Inventory datasets, "estuarine intertidal emergent" classification (U.S. Fish and Wildlife Service, 2018). b) Points were placed along the marsh-forest boundary using methods detailed in Molino, Defne, et al., (2021), and elevation values extracted at each point from the Chesapeake Bay Coastal National Elevation Database. c) Median elevation of marsh-forest boundaries for 81 Hydrologic Unit (HUC) 10; 5 additional units have no color as there were <100 points in that unit so a median elevation was not determined. Median elevation was taken from all points within each HUC. Reproduced from Molino et al. 2022.

Figure 2. Median values for a) tidal range, b) salinity, and c) average slope within the 68 watersheds in the Chesapeake Bay used in the linear model. Five watersheds have no color as there were insufficient source data. Salinity and slope maps reproduced from Molino et al. 2022. Tidal data obtained from National Oceanic and Atmospheric Administration (NOAA) VDatum (vdatum.noaa.gov). Salinity values based on model output provided by St-Laurent et al. 2020.

Figure 3. Median threshold elevation for each Hydrologic Unit (HUC) 10 watershed in Chesapeake Bay versus a) tidal range, b) salinity, and c) slope. In each panel, the highlighted watersheds correspond to the paired-watershed analysis presented in Figure 4. The locations of each watershed are shown in Supporting Information Figure S1.

Figure 4. a) Probability density estimate for all spatially explicit threshold elevation points within the study region. b-d) Paired-watershed analysis comparing the elevation distribution of representative watersheds, where 2 of 3 variables are similar. Panel b compares probability density estimates for two watersheds with high (1.08 m) and low (0.19 m) tidal ranges. Panel c compares probability density estimates for two watersheds with high (31.3 ppt) and low (2.1 ppt) salinities. Panel d compares probability density estimates for two watersheds with high (3.1%) and low (2.7 %) slope. In panels b-d, vertical lines represent median threshold elevation for each watershed, and are significantly different from each other. The locations of each watershed are shown in Supporting Information Figure S1. Tidal data obtained from the National Oceanic and Atmospheric Administration (NOAA) VDatum. Salinity data from St. Laurent et al., 2021.

Figure 5. Comparisons of predicted marsh migration area using the single value (orange), National Oceanic and Atmospheric Administration (NOAA) (teal), and spatially explicit (dark purple) approaches in North Landing River, Virginia, USA (panel e). a) Overlay of single value and spatially explicit marsh migration projection methods with 0.45 m of sea level rise (SLR) and b) 1.22 m of SLR. c) Overlay of NOAA and spatially explicit marsh migration projection methods with 0.45 m of SLR and d) 1.22 m of SLR. NOAA marsh migration area estimates were quantified using data downloaded from NOAA Sea Level Rise Viewer (https://coast.noaa.gov/slrdata/). Spatially explicit marsh migration areas were obtained from Molino et al. 2022. Gray areas are delineated as estuarine emergent marsh by the National Wetlands Inventory (U.S. Fish and Wildlife Service, 2018). The spatially explicit approach (purple) appears to cover a greater area in panels a-b as the projections start at the median threshold elevation (0.32 m) as opposed to the single value approach (orange) which starts at highest astronomical tide (0.61 m). See Table 2 for quantified areas for each method.

Figure 6. Local drivers (land use, hydrology, microtopography) influence elevation of transition from marsh to upland; a) levee built at boundary between marsh and agricultural land (Atlantic lagoons, Virginia, USA); b) band of narrowleaf cattail (*Typha langustifolia*) at marsh-forest boundary indicative of freshwater seepage (Atlantic lagoons, VA, USA); c) loblolly pine trees (*Pinus taeda*) growing on mound (Atlantic lagoons, VA, USA). Atlantic lagoons located in watersheds 37-39 in Supporting Information Figure S1. Photo a taken by G.C. Levins and photos b-c taken by G.D. Molino.

Table 1. Input variables for the linear model explaining forest retreat at the Hydrologic Unit (HUC) 10 watershed scale. Significant variables in italics. Variables with a p-value greater than 0.1 labeled NS (not significant) and the coefficient labeled NA (not applicable). Processed variable input values for each watershed are published in the Environmental Data Repository (Molino et al., 2023). Links to original raw data are included here and cited in text. Full source citations in References.

Variable	p-value	Coefficient	Resolution	Source
Tidal range	*0.001*	*0.2264*	*400 m*	*NOAA VDatum*
Surface salinity	*0.000*	*0.0083*	*600 m*	*St-Laurent et al., (2020)*
Average slope	*0.003*	*0.1304*	*30 m*	*Molino et al., (2020)*
Topographic position index (TPI)	NS	NA	30 m	Derived from Danielson & Tyler, (2016)
Distance to open water	NS	NA	Polygon	Water extent from Chesapeake Conservancy, (2018)
Watershed area	NS	NA	Polygon	USGS, (2020)
Annual temperature	NS	NA	4000 m	PRISM Climate Group, (2019)
Annual precipitation	NS	NA	4000 m	PRISM Climate Group, (2019)
Growing degree days	NS	NA	4000 m	PRISM Climate Group, (2019)
Hurricane Isabel max inundation depth	NS	NA	100-300 m	Molino, Defne, et al., (2021) (originally modeled by ADCIRC)
Hurricane Isabel inundation duration	NS	NA	100-300 m	Molino, Defne, et al., (2021) (originally modeled by ADCIRC)
Historic surface water occurrence	NS	NA	25 m	Global Surface Water Explorer (Pekel et al., 2016)
Change in surface water occurrence	NS	NA	25 m	Global Surface Water Explorer (Pekel et al., 2016)
Normalized difference water index (NDWI)	NS	NA	30 m	Landsat-8 acquired from Earth Explorer

Table 2. Variation in current threshold elevation and projected marsh migration as determined with three different approaches. In the single value approach, a single threshold elevation is determined using a regionally averaged highest astronomical tide (HAT) that is applied to the entire region to predict marsh migration (e.g. Mitchell et al. 2020). In the National Oceanic and Atmospheric Administration (NOAA) approach, marsh migration is quantified using data downloaded from the NOAA Sea Level Rise Viewer (https://coast.noaa.gov/slrdata/), and is based on modeled changes in tidal datum alone. The spatially explicit method is based on a threshold elevation calculated for each watershed (Molino et al., 2022), which implicitly includes spatial variability in the biophysical factors considered in the present study (i.e. salinity, tidal range, and slope). All elevations in m North Atlantic Vertical Datum of 1988. Sea level rise (SLR) scenarios based on Sweet et al. 2017. Marsh migration areas within the Hydrologic Unit (HUC) 1 watershed are depicted in Figure 5. Location of both watersheds within the Chesapeake Bay can be found in Supporting Information Figure S1.
[a]Mitchell et al. (2020). [b]Molino et al. (2022).

Virginia Atlantic Lagoons (HUC38)	Single value	NOAA	Spatially explicit
Threshold Elevation (m)	0.61[a]	NA	1.05[b]
Migration area (km^2) – Low SLR (0.45 m)	17.81	15.04	16.16
Migration area (km^2) – Intermediate SLR (1.22 m)	43.23	35.37	37.70
North Landing River (HUC1)	Single value	NOAA	Spatially explicit
Threshold Elevation (m)	0.61[a]	NA	0.32[b]
Migration area (km^2) – Low SLR (0.45 m)	15.22	74.24	61.32
Migration area (km^2) – Intermediate SLR (1.22 m)	40.45	92.73	83.90

Figure 1.

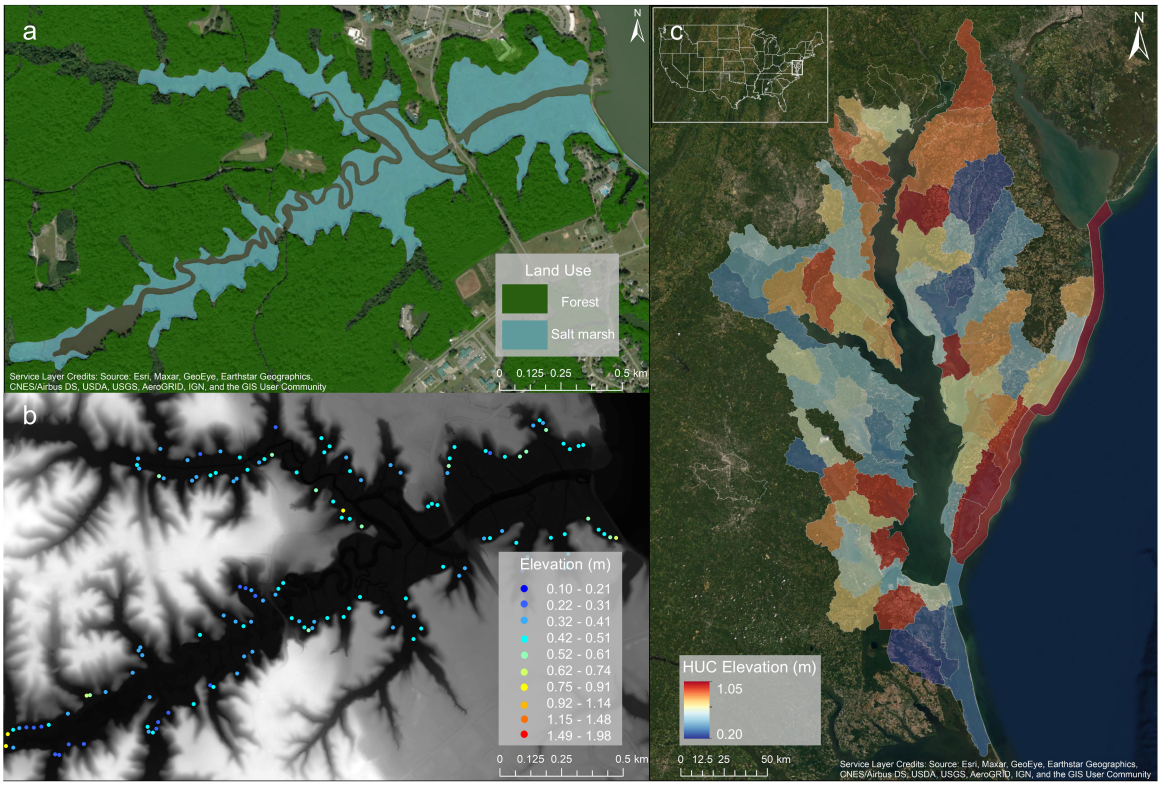
a
N
Land Use
Forest
Salt marsh
0 0.125 0.25 0.5 km
Service Layer Credits: Source: Esri, Maxar, GeoEye, Earthstar Geographics, CNES/Airbus DS, USDA, USGS, AeroGRID, IGN, and the GIS User Community
b
Elevation (m)
0.10 - 0.21
0.22 - 0.31
0.32 - 0.41
0.42 - 0.51
0.52 - 0.61
0.62 - 0.74
0.75 - 0.91
0.92 - 1.14
1.15 - 1.48
1.49 - 1.98
0 0.125 0.25 0.5 km
c
N
HUC Elevation (m)
1.05
0.20
0 12.5 25 50 km
Service Layer Credits: Source: Esri, Maxar, GeoEye, Earthstar Geographics, CNES/Airbus DS, USDA, USGS, AeroGRID, IGN, and the GIS User Community

Figure 2.

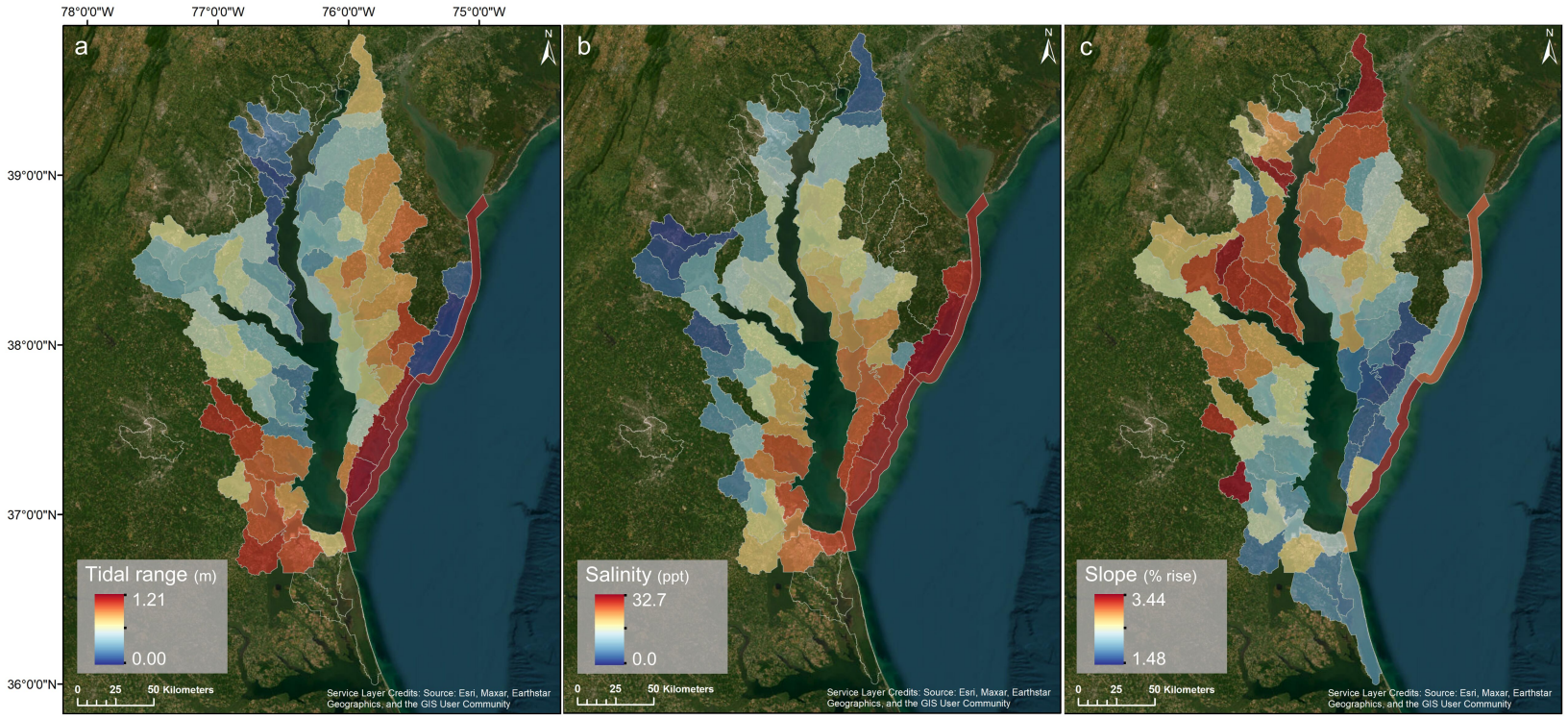
78°0'0"W
77°0'0"W
76°0'0"W
75°0'0"W
39°0'0"N
38°0'0"N
37°0'0"N
36°0'0"N
a
N
Tidal range (m)
1.21
0.00
0 25 50 Kilometers
Service Layer Credits: Source: Esri, Maxar, Earthstar Geographics, and the GIS User Community
b
N
Salinity (ppt)
32.7
0.0
0 25 50 Kilometers
Service Layer Credits: Source: Esri, Maxar, Earthstar Geographics, and the GIS User Community
c
N
Slope (% rise)
3.44
1.48
0 25 50 Kilometers
Service Layer Credits: Source: Esri, Maxar, Earthstar Geographics, and the GIS User Community

Figure 3.

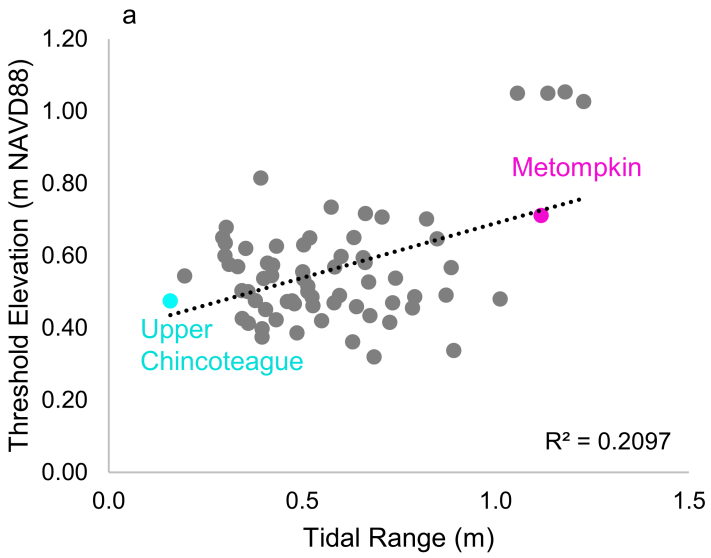
a
Threshold Elevation (m NAVD88)
1.20
1.00
0.80
0.60
0.40
0.20
0.00
Metompkin
Upper
Chincoteague
R² = 0.2097
0.0
0.5
1.0
1.5
Tidal Range (m)

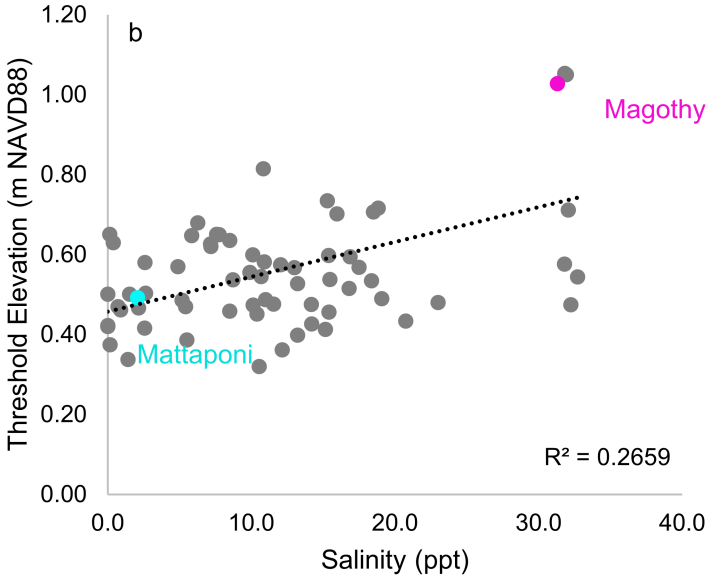
b
Threshold Elevation (m NAVD88)
1.20
1.00
0.80
0.60
0.40
0.20
0.00
Magothy
Mattaponi
R² = 0.2659
0.0
10.0
20.0
30.0
40.0
Salinity (ppt)

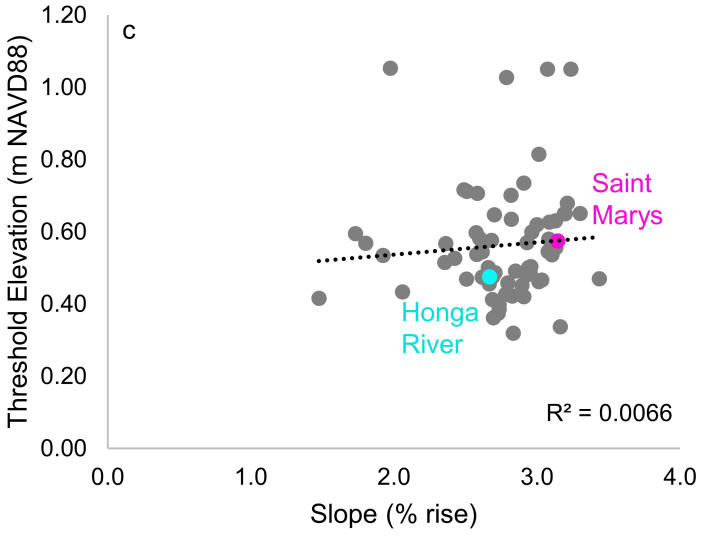
c
Threshold Elevation (m NAVD88)
1.20
1.00
0.80
0.60
0.40
0.20
0.00
Saint
Marys
Honga
River
R² = 0.0066
0.0
1.0
2.0
3.0
4.0
Slope (% rise)

Figure 4.

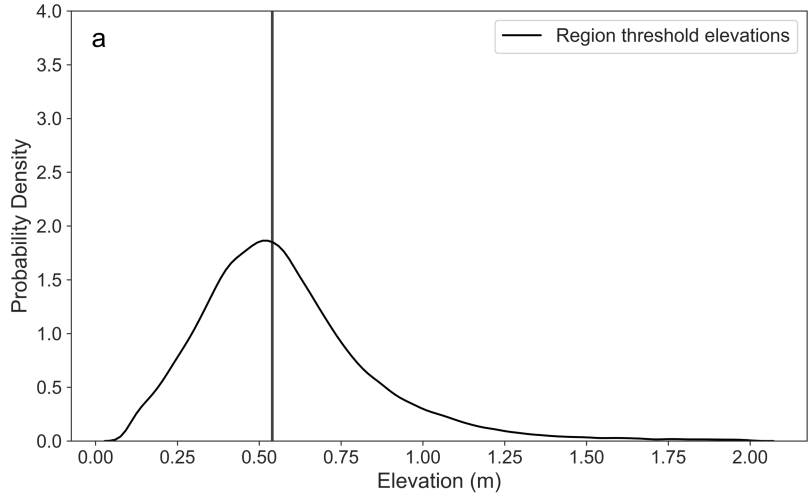
a
Region threshold elevations
Probability Density
Elevation (m)

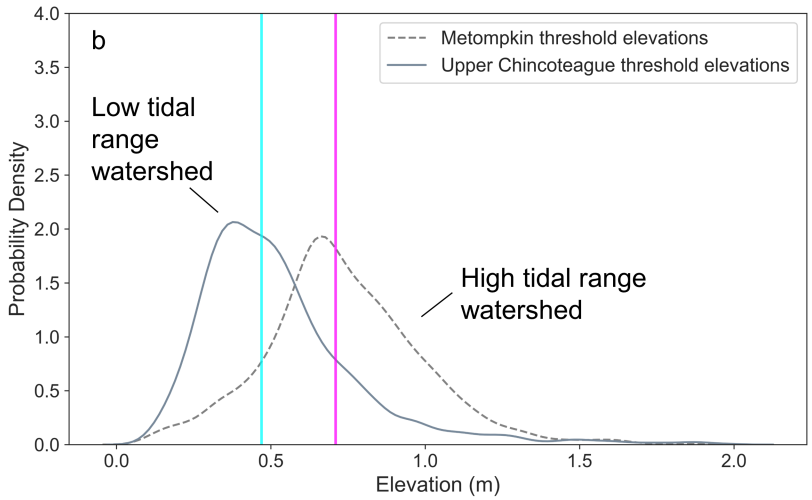
b
Metompkin threshold elevations
Upper Chincoteague threshold elevations
Low tidal range watershed
High tidal range watershed
Probability Density
Elevation (m)

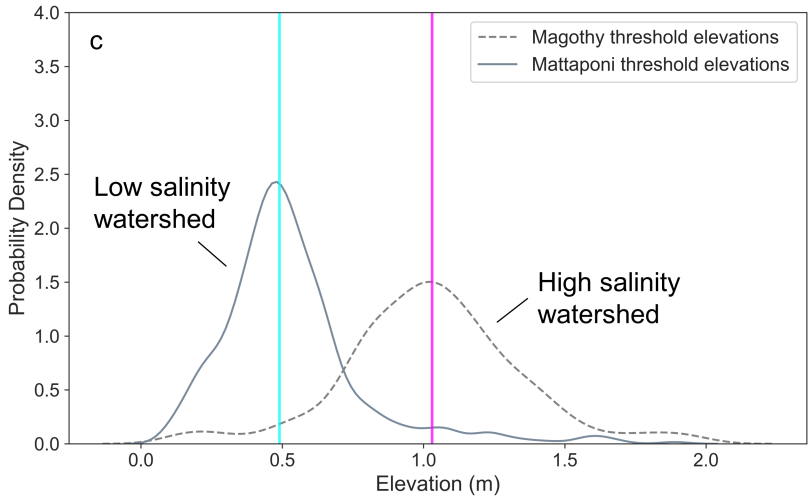
c
Magothy threshold elevations
Mattaponi threshold elevations
Low salinity watershed
High salinity watershed
Probability Density
Elevation (m)

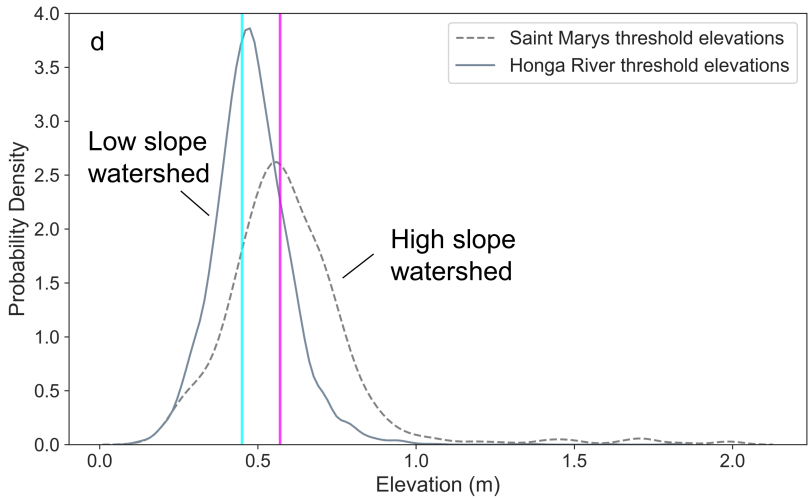
d
Saint Marys threshold elevations
Honga River threshold elevations
Low slope watershed
High slope watershed
Probability Density
Elevation (m)

Figure 5.

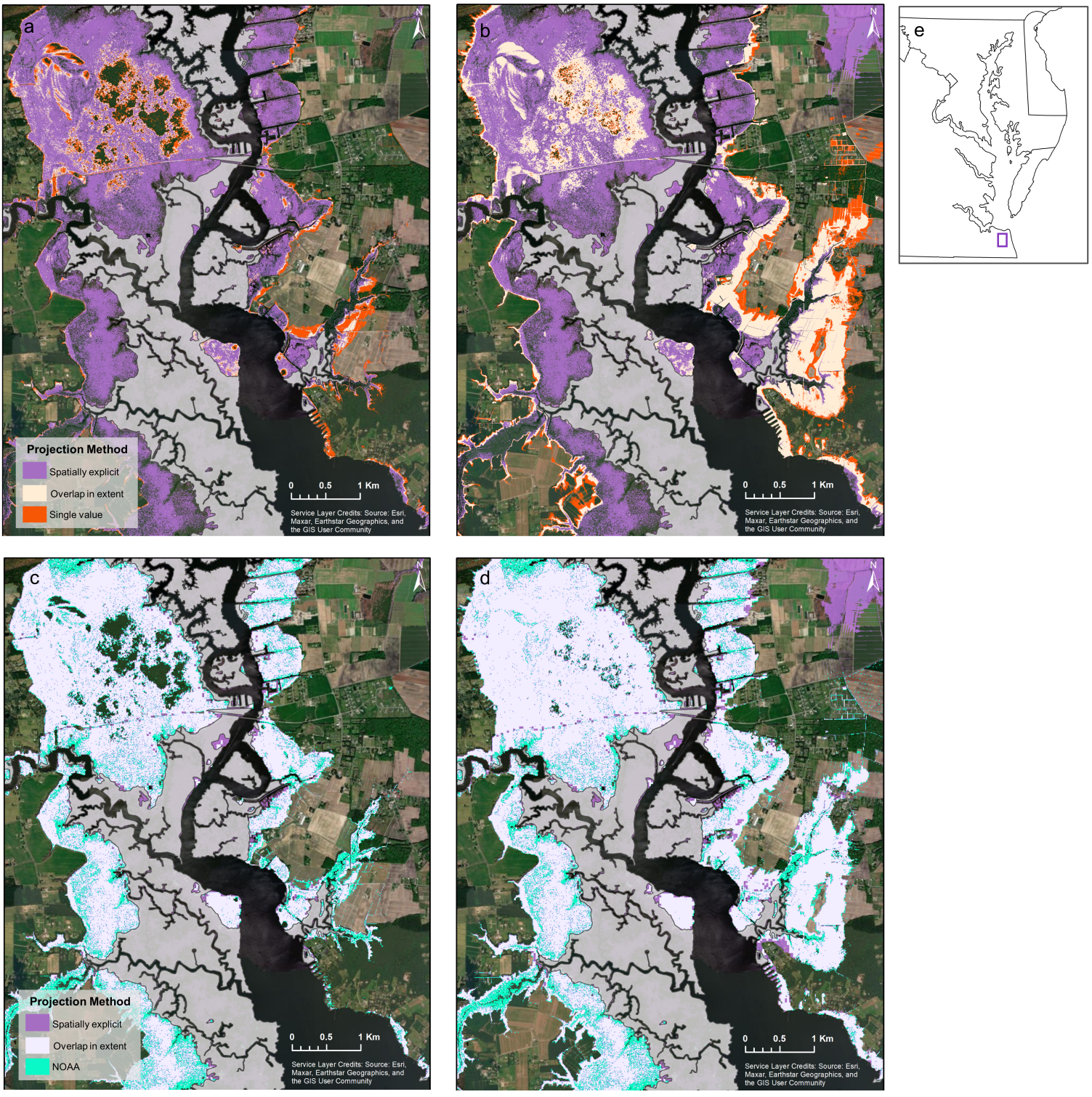
a
b
c
d
e
N
Projection Method
Spatially explicit
Overlap in extent
Single value
NOAA
0 0.5 1 Km
Service Layer Credits: Source: Esri, Maxar, Earthstar Geographics, and the GIS User Community

Figure 6.


a


b


c